

Role of Middle-Ear Inertial Component of Bone Conduction in Chinchilla

by

David Chhan

B.S., University of Massachusetts Lowell (2010)

Submitted to the Department of Electrical Engineering and Computer
Science

in partial fulfillment of the requirements for the degree of

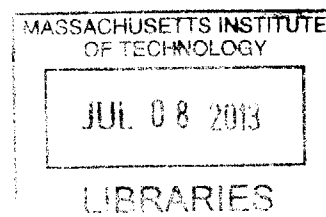
Master of Science in Electrical Engineering and Computer Science

at the

MASSACHUSETTS INSTITUTE OF TECHNOLOGY

June 2013

ARCHIVES



© Massachusetts Institute of Technology 2013. All rights reserved.

Author
Department of Electrical Engineering and Computer Science
May 7, 2013

Certified by
John J. Rosowski
Professor of Otology and Laryngology, & Health Sciences and
Technology, HMS
Thesis Supervisor

Accepted by
Leslie A. Kolodziejcki
Chairman, Department Committee on Graduate Theses

Role of Middle-Ear Inertial Component of Bone Conduction in Chinchilla

by

David Chhan

Submitted to the Department of Electrical Engineering and Computer Science
on May 7, 2013, in partial fulfillment of the
requirements for the degree of
Master of Science in Electrical Engineering and Computer Science

Abstract

Bone conduction describes the mechanisms that produce a hearing sensation when the skull bones are subjected to vibration. Multiple components and pathways have been suggested to contribute to total bone-conducted sound. They include outer-ear cartilaginous wall compression, middle-ear inertia, fluid inertia, cochlear capsule compression and soft-tissue conduction. Due to the complexity of the possible interactions within these components and pathways, the true stimulus to the inner ear is not fully understood nor has it been adequately quantified. In this thesis work, we examined the relationship between inner-ear sound pressures and its sensory response in addition to determining the relative significance between the outer, middle and inner ear mechanisms that are prominent in bone conduction hearing in chinchilla. Using both mechanical and physiological recording techniques, we measured cochlear responses in chinchilla before and after interruption of the middle-ear ossicular system in both air conduction (AC) and bone conduction (BC) stimulation.

Our data suggest that differential intracochlear sound pressure is the driving source to the sensory response of the inner ear in AC and BC. Compared to those in AC, inner-ear sound pressure measurements in BC provide evidence of multiple mechanisms in BC process. After middle ear interruption, pressures in scala vestibuli P_{SV} and scala tympani P_{ST} drop by as much as 40 dB in AC, but only decrease in P_{SV} by 10 dB, with almost no change in P_{ST} in BC. The difference in the change of both P_{SV} and P_{ST} in BC compared to AC suggest the main mechanisms that drive the inner ear response in BC are not derived from the outer ear or middle ear but the inner ear.

Thesis Supervisor: John J. Rosowski

Title: Professor of Otology and Laryngology, & Health Sciences and Technology, HMS

Acknowledgments

First and foremost, I would like to express my utmost thank and deepest gratitude to my advisor John Rosowski for his continuing support and guidance throughout this research project. His mentorship is beyond the technical work presented here and his dedication to teaching and caring for his students deserve much recognition. I learnt a great deal being with him over the past years. I also profoundly thank my undergraduate advisor Professor Thompson who at the University of Massachusetts Lowell (UML) has given me many valuable advice. Professor Chandra first introduced me to the world of scientific research and allowed me to get involved in a few projects in her laboratory at UML. Her generosity and discipline impacted me greatly.

I want to acknowledge the people in the Middle-Ear group and Eaton-Peabody Laboratory at the Massachusetts Eye and Ear Infirmary for their support. I cannot thank Melissa enough for her help in animal surgery and experimental preparation. I am also grateful to Heidi and Mike for showing me how to make pressure transducers. Tao and Gabby are always there for me when needed. My classmates: Jon Sellon, Luke Shaheen, Jonathon Whitton, Samiya Alkhairy, Will Feng and Goldie Mehraei, have been great partners since I started the SHBT program.

Finally, my parents, who always seek out the best opportunities for their children including their decision to move to the US in late 2006, are the source of my inspiration and hard-work. I am grateful for their encouragement and high expectations that pushed me to be who I am today.

Contents

1	Introduction	11
1.1	Anatomy of the Peripheral Auditory System	12
1.2	The Conduction of Airborne Sound	14
1.3	The Conduction of Bone Vibrations	15
1.4	Vibration Modes, Pathways and Components in Bone Conduction . .	16
1.4.1	Ear-Canal Cartilaginous Wall Compression Mode	16
1.4.2	Middle-Ear and Inner-Ear Fluid Inertia Mode	17
1.4.3	Inner-Ear Wall Compression and Non-Osseous Soft Tissue Fluid Pathways	17
1.5	Aims of This Study	19
1.5.1	Specific Aim 1: Determine the Relationship between Inner-Ear Sound Pressures and Physiological Cochlear Responses	20
1.5.2	Specific Aim 2: Quantify the Contribution of the BC Stimulus Components that Depend on Ossicular Motion by Interruption of the Incudo-Stapedial Joint	21
2	Material and Methods	23
2.1	Fiber-Optic Pressure Sensors	24
2.1.1	Sensor Tip with Gold-Coated Diaphragm Construction	24
2.1.2	Fiber-Optic Pressure Sensor Probe Assembly	24
2.1.3	Calibration: A Test of Sensitivity and Stability	25
2.2	Cochlear Potentials	27
2.3	Animal Preparation	27

2.4	Acoustic and Vibration Stimuli	28
2.5	Experimental Procedure	29
3	Results	31
3.1	Inner-Ear Responses to Air Conduction and Bone Conduction: ΔP and CP	32
3.1.1	Intracochlear Sound Pressure Measurements in AC	33
3.1.2	Intracochlear Sound Pressure Measurements in BC	34
3.1.3	Comparison of CP and ΔP in AC and BC	37
3.2	Effects of Middle-Ear Ossicular Chain Interruption in AC and BC . .	40
4	Discussion	45
4.1	Is the Differential Intracochlear Sound Pressure the Driving Source to the Sensory Response of the Inner Ear in AC and BC?	45
4.2	Evidence for the Contribution of Multiple Mechanisms to the BC re- sponse in the Normal Measurements	46
4.3	Evidence for the Contribution of Inner Ear Mechanisms to the BC response in the Measurements Made After Middle Ear Interruption .	47
4.4	Comparison of Intracochlear Sound Pressure of the Current Study to Other Studies	49
5	Conclusions	51

List of Figures

1-1	Anatomy of the peripheral auditory system (skidmore.edu).	12
1-2	Schematic of the cochlea (en.wikipedia.org).	14
1-3	Schematic of the compressional BC mechanism after Békésy [22].	18
2-1	Schematic of the fiber-optic pressure sensor assembly.	25
2-2	Schematic of a calibration setup.	26
2-3	Frequency dependence and sensitivity of a representative sensor before and after an experiment.	26
2-4	Schematic of the animal preparation and experimental setup.	28
3-1	Magnitude of CP response curves evoked by AC and BC at different frequencies in one experiment. The abscissa describes the voltage input to the AC and BC transducer in terms of dB re 1 volt. Linear growth of CP was generally observed with AC sound stimuli of less than 80 dB SPL, and BC vibratory stimuli of less than 35 dB mm/s ²	32
3-2	Normalized P_{SV} , P_{ST} , CP and ΔP in AC in nine individual animals. The red lines illustrate the means and gray-shaded area illustrates ± 1 standard deviation around the mean. All measurements are normalized by the sound pressure in the ear canal; panels A, B & D plot a dimensionless ratio of two pressures, and panel C plots a dB representation of the ratio of V/Pa.	33
3-3	Ratio of P_{ST} over P_{SV} in AC in the nine individual animals. The red line illustrates the mean and the gray-shaded area illustrates ± 1 standard deviation around the mean.	34

3-4	P_{SV} , P_{ST} , CP and ΔP in BC in nine individual animals. The red lines illustrate the means and the gray areas ± 1 standard deviation around the mean. All panels represent the ratio of the measured pressure or CP and the voltage drive to the BC stimulator.	35
3-5	Ratio of P_{ST} over P_{SV} in BC in the nine individual animals. The red line illustrates the mean and the gray-shaded area illustrates ± 1 standard deviation around the mean.	36
3-6	A measure of the velocity of the skull evoked by the BC stimulus in one experiment. The velocity was measured with a one-dimensional laser Doppler vibrometer. The vibrometer was positioned to be sensitive to a combination of lateral and up and down skull motions. The magnitude of the velocity falls off below 0.4 kHz and above 4 kHz.	36
3-7	Cochlear potential CP and differential intracochlear sound pressure ΔP measurements in AC and BC in ear CH03. The CP data have been scaled to match the pressure data.	37
3-8	Comparison of magnitude of cochlear potential CP and differential intracochlear sound pressure ΔP in AC and BC in nine ears. The CP data have been scaled to best match the pressure data. The R values are discussed below.	38
3-9	Inner ear responses P_{SV} , P_{ST} , CP , and ΔP in AC and BC before and after IS-joint interruption from one experiment (Ear CH15).	41
3-10	Effects of incudo-stapedial joint interruption in AC on P_{SV} , P_{ST} and ΔP for 8 ears and CP for 12 ears including the mean and standard deviation.	42
3-11	Effects of incudo-stapedial joint interruption in BC on P_{SV} , P_{ST} and ΔP for 8 ears and CP for 12 ears including the mean and standard deviation.	43
4-1	P_{SV} , P_{ST} , and ΔP in AC in comparison with previous studies.	50

Chapter 1

Introduction

The auditory-system involves two main stages of signal processing, the peripheral and central auditory systems. The peripheral auditory system converts mechanical vibration of the air molecules to neuro-electrical signals that are transmitted to the brain; the central auditory system processes those neural signals to allow judgements of the behavioral importance of sound, e.g. its meaning and direction. The focus of this thesis work is on the peripheral auditory system, including the outer, middle and inner ears, and mainly deals with the acoustic and mechanical transfer of sound between these components. Two major sound stimulus pathways exist: 1) air conduction, the collection and conduction of airborne sound through the periphery, and 2) bone conduction, the coupling of vibratory signals to the sensory cells within the inner ear. Stimulation of the ear by either path produces similar stimulation of the auditory sensors within the inner ear and common auditory sensations. However, the mechanisms that produce this stimulation are quite different in the two pathways. In this section, we will discuss the anatomy and function of the different components of the peripheral auditory system. We will also briefly describe the mechanisms of air conduction versus bone conduction before introducing the specific aims of this study.

1.1 Anatomy of the Peripheral Auditory System

The major peripheral components are schematized in Figure 1-1.

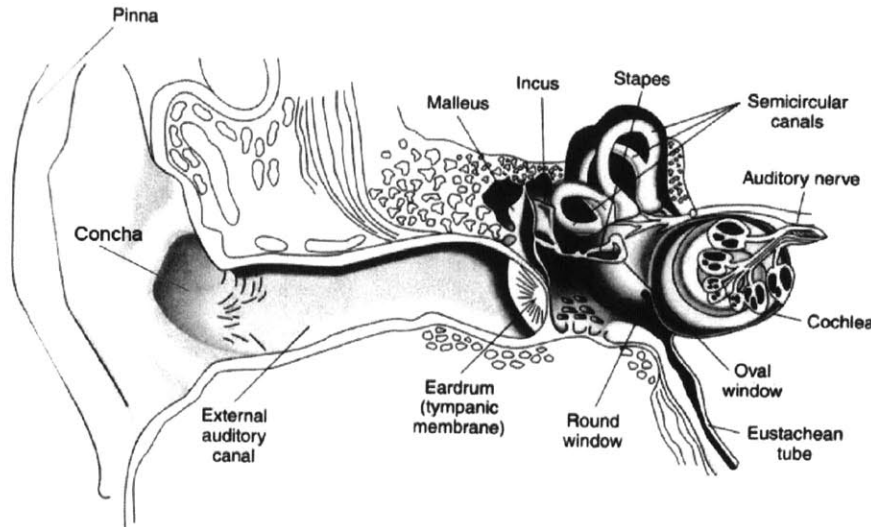


Figure 1-1: Anatomy of the peripheral auditory system (skidmore.edu).

The outer ear is subdivided into a pinna, concha and external auditory canal and is terminated by the tympanic membrane, or eardrum. The pinna or the ear flap is a cartilaginous structure that serves as a sound collector directed to the ear canal. It also plays a role in spectral transformations that assist in sound localization in the vertical plane [1]. The concha is the hollow depression near the entrance of the ear canal. The ear canal is a 2-3 mm long tube-like structure whose outer 1/3 is supported by cartilage and the inner 2/3 is embedded in the temporal bone. The external ear canal can be considered as a passive sound transformer [1] in which sound pressure measured near the surface of the tympanic membrane is higher than at the entrance of the ear canal. The external sound pressure gain can be as large as 20 dB near 4 kHz [2].

The ear canal is terminated by a cone-shaped membrane called the tympanic membrane (TM). The TM functions as an acoustical-to-mechanical transformer that converts airborne sound energy in the ear canal to mechanical vibration of the middle-ear ossicles. Anatomically, the TM is attached to the manubrium (the handle) of the

malleus at the umbo (at the center of the TM) and near the TM rim. The attachment of the TM to the manubrium appears to draw the center of the TM into the tympanic cavity. In some mammals, including the chinchilla, the middle-ear or tympanic cavity is extended by a thin-walled bony capsule called the “bulla”.

In this air-filled cavity are the three tiny middle-ear bones: malleus, incus and stapes, whose Latin names mean hammer, anvil, and stirrup respectively. The ossicles are coupled together and supported by ligaments and tendons. There are two ligamentous joints, the incudo-malleolar joint (between the head of the malleus and the body of the incus) and the incudo-stapedial joint (between the lenticular process of the incus and the head of the stapes). Sound pressure in the ear canal sets the TM into motion that is transmitted to the middle-ear ossicles. In a simplistic view, the malleus and incus rotate as rigid bodies about an axis defined by supporting ligaments; this motion produces in-and-out piston-like motion of the stapes within the oval window to the inner ear. The three middle-ear ossicles together act as a mechanical lever that helps match the low impedance of the air at the external ear canal to the high impedance of the water-like fluids in the inner ear. This impedance matching is greatly assisted by the 20 times difference in the area of the TM and the stapes footplate, where this area difference produces a hydraulic lever that trades a drop in sound-induced volume displacement between the TM and the footplate for an increase in sound pressure.

Movement of the middle-ear ossicles can be reduced by two muscles that act to stiffen the middle-ear mechanism: the tensor tympani (attached to the manubrium of the malleus) and the stapedius (attached to the head of the stapes). These muscles contract in response to loud sounds that can excessively vibrate the middle ear, thus reducing the response transmitted to the inner ear. This protective function is called the acoustic reflex.

The last link of the ossicular chain, the stapes, is connected to the cochlea (the auditory portion of the inner ear) at the oval window by an annular ligament. The oval window is an entrance to the spiral-shaped cochlea in which three lymph-filled chambers surround the sensory structures that transform sound pressures within the

lymphs to sensory potentials and action potentials on the auditory nerve. The sensory components are housed in the organ of corti located in the scala media that is sandwiched between scala vestibuli and scala tympani. The oval window is placed in the basal end of scala vestibuli. Scala vestibuli and scala tympani are linked at the helicotrema in the apex of the cochlea. The basal end of scala tympani is terminated by the round window which provides a low-impedance pressure release that permits the back and forth motion of the scalae fluids when sound causes motion of the stapes (Fig. 1-2). The horizontal dashed line of Figure 1-2 indicates a fluid path in the two chambers.

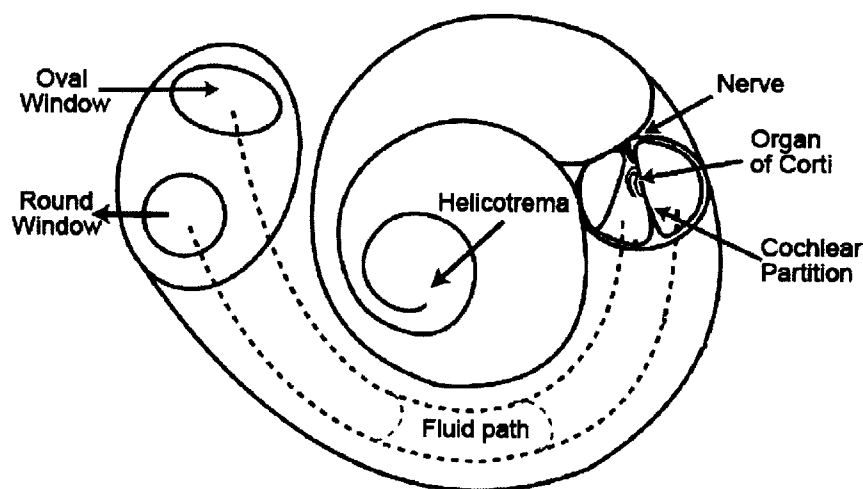


Figure 1-2: Schematic of the cochlea (en.wikipedia.org).

1.2 The Conduction of Airborne Sound

“Air conduction” refers to the conduction of air-borne sound in the ear canal through the middle ear to the inner ear. This is the most common mode for sound energy to reach the inner ear. The process starts with sound pressure in the ear canal. The associated compression and rarefaction generates motion of the TM which sets the three middle-ear ossicles into vibration. Vibration of the stapes causes motion of the fluids in the cochlea. The motion in turn produces a pressure difference across the cochlear partition where the basilar membrane (BM) and organ of corti are located.

The pressure difference leads to the initiation of traveling waves along the basilar membrane. A sound of certain frequency produces a vibration of the basilar membrane at a certain place, thus there is a ‘place map’ between frequency and location of maximum vibration within the inner ear. As a result, the cochlea is often described as a frequency analyzer where high-frequency sound excites the basilar membrane at the base and low-frequency sound excites the basilar membrane at the apex. The mechanical vibration of the basilar membrane stimulates the hair cells in the organ of corti, which produce sensory potentials that evoke action potentials in the dendrites of the auditory nerve. The electrical action impulses are then transmitted to the brain.

1.3 The Conduction of Bone Vibrations

In the audiology clinic, bone conduction (BC) describes a collection of mechanisms that produce a hearing sensation in response to vibration of the bones of the skull. Early investigations of the sound-conduction processes in bone conduction were largely driven by clinical application. Use of BC hearing in clinical practice dates back to the 19th century when Weber and Rinne developed hearing tests that employed a tuning fork to separate conductive (middle ear based) and sensorineural (inner ear based) hearing losses [3]. Such a separation depended on the hypothesis that the conduction of skull vibrations to the inner ear was independent of the middle ear. Patients who showed a decrease in auditory sensitivity to tuning forks held in air near the ear canal (an AC stimulus), but had normal sensitivity to tuning forks coupled to the bone near the ear (a BC stimulus) had a conductive hearing loss; while patients with sensory neural hearing loss showed an equal decrease in sensitivity to tuning forks held in air and coupled to the skull.

Despite the early use of bone conduction as a tool in hearing test, its mechanisms were not investigated at any depths until the work of Bárány [21], Wever and Lawrence [29], Békésy [22], Huizing [23], and Tonndorf [25]. Their clinical observations and experimental results have established the basis of current theories of how

bone vibration is perceived as sound.

1.4 Vibration Modes, Pathways and Components in Bone Conduction

According to Wever and Lawrence [29], there are three major modes that contribute to bone-conduction hearing. The modes correspond to the components of the auditory periphery and pathways in which bone vibration transfers to fluid motion in the cochlea. In brief, the first mode relates to sound energy that radiates into the ear canal through compression of the cartilaginous ear-canal wall. The second is a translatory mode that causes ossicular motion due to differences between the inertia of the skull, the ossicles in the middle ear and the fluids within the inner ear. The third is a compressional mode in which motion of the cochlear fluids results from the compression and expansion of the bony cochlear capsule.

1.4.1 Ear-Canal Cartilaginous Wall Compression Mode

Vibration of the skull and attached jaw produces vibrations of the cartilaginous ear canal that rarify and compress the air within the canal. The resultant sound energy induced in the ear canal produces motion of the tympanic membrane. Artifactual acoustic radiation from the vibratory source, so-called the airborne bone conduction, can also alter the sound pressure in the ear canal. In this mode, the pathway from TM motion to the cochlea is the same as in air-conducted sound where the ear canal sound pressure is produced by an external source. While the contribution of ear-canal compression to bone-conducted sound is small when the canal is open, occluding the ear canal increases the sound pressure produced by wall vibrations and leads to increases in the loudness of the perceived sound. This observation leads to naming this pathway ‘the occlusion effect’ [4].

1.4.2 Middle-Ear and Inner-Ear Fluid Inertia Mode

The translatory motion of the head induces relative motion between the head and the coupled ossicles and inner-ear fluids. These relative motions result because of differences in the inertia of these structures, together with the elastic coupling of the ligaments that support the ossicles in the skull and the cochlear windows that restrain the fluid in the inner ear. From a mechanical standpoint, the middle-ear ossicles and the fluid of the inner ear act as free masses, which are loosely attached to the head by ligaments, tendons and the TM which act as mechanical springs. At low frequency, below the middle-ear resonance frequency of 1-2 kHz, the ossicles and the fluids of the inner ear vibrate in phase with the bones surrounding the middle and inner ear. At higher frequencies; however, vibration of the bone and the middle-ear ossicles are no longer in phase thus causing a relative motion that stimulates the cochlear partition. As pointed out by Bárány [21] this stimulation depends on the direction of vibration, where the anatomy of the ear is most sensitive to side-to-side shaking of the head.

1.4.3 Inner-Ear Wall Compression and Non-Osseous Soft Tissue Fluid Pathways

In the compressional mode, the cochlear capsule undergoes compression and expansion. Figure 1-3 illustrates this mechanism at work. In the figure, the cochlea is uncoiled and viewed as a rectangular chamber constrained by bone and the flexible oval window (OW) and round window (RW) to the left. The chamber is split in two by the cochlear partition which separates scala vestibuli (SV) on the top and scala tympani (ST) on the bottom (Fig. 1-3 A). The compressions and rarefactions of the bone around the cochlea induce volume changes in the inner ear spaces. These volume changes in the presence of the flexible cochlear windows produce motion of the nearly incompressible cochlear fluids. Differences in the impedance of the two flexible cochlear windows produce a differential fluid flow in the cochlea that can set up traveling wave patterns just as when the cochlea is stimulated by air conducted sound (Fig. 1-3 B). Differences in motion of the two scalae can be enhanced by asymmetries

in inner-ear structure and by compressible structures within the inner ear (Fig. 1-3 C).

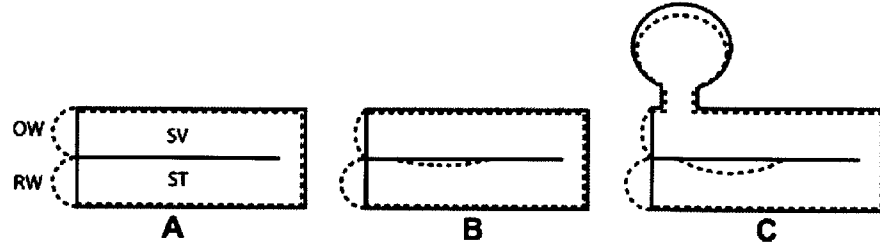


Figure 1-3: Schematic of the compressional BC mechanism after Békésy [22].

The non-osseous soft tissue fluid pathway describes the stimulation of the inner ear fluid via sound conduction through the soft tissues and body fluids that surround and penetrate the bony inner ear, such as vibration of the brain and cerebro-spinal fluid [5]. This mechanism has features similar to cochlear compression in that it allows a differential flow of lymphs within the inner ear. The difference is that the lymph flow is produced by vibration sources outside of the bony inner ear.

The three vibratory modes with their involved components and pathways coexist and independently contribute to bone-conducted sound. Due to the complex interaction of these multiple pathways, the relative contributions of each of the pathways to bone-conducted sound are still poorly understood. Bárány [21] and Huizing [23] stressed the importance of middle-ear inertia as the dominant mode in bone conduction while Tonndorf [24] [25] argued that the compressional mode is more significant. More recently, Stenfelt and coworkers [6] have argued for the primacy of inner-ear fluid inertia. What seems to be agreed upon is their admission of the complexity of bone conduction stimulation.

Recent work on bone conduction in both clinical and experimental settings suggests the contribution of the different stimulus pathways are highly frequency dependent. Stenfelt and coworkers suggest middle-ear and inner-ear fluid inertia contribute to the perception of bone-conducted sounds between the frequencies of 1.5 and 3.5 kHz [7]. They compared ossicle displacements at hearing thresholds for both AC and

BC and showed that between 1.5 and 3.5 kHz the motions in both cases are within 5 dB indicating middle-ear ossicular motions contribute to BC perception in that frequency range. They also found a decrease in stapes velocity after incudo-stapedial joint interruption in BC stimulation [8].

Evidence consistent with a significant cochlear compression mode was presented by Songer and Rosowski who studied superior canal dehiscence syndrome (SCD) [10]. Patients with SCD [9] present not only with vestibular symptoms, but also auditory symptoms that include improved sensitivity to bone conducted stimuli along with decreased sensitivity to air conducted sound. Rosowski and coworkers suggest a model of SCD effects that includes inner ear compression at frequencies below 1 kHz. Such a model is consistent with their animal studies on the effects of SCD syndrome in both AC and BC sound [10]. Their model suggests SCD acts like a third window shunting acoustic energy from the ear to the braincase thus reducing hearing sensitivity to air conducted sound. Such shunting allows relative motions of the fluids in scala vestibuli and tympani, and is thought to increase relative fluid flow in bone conduction and improve hearing sensitivity to BC sound.

1.5 Aims of This Study

Unlike air conduction, where one distinct sound pathway has been identified, the multiple conduction pathways in bone conduction and their interaction are poorly understood. In particular, the frequency range and the relative importance of each pathway to the total BC sensation are not well described. The overall goal of this project is to improve our understanding of the contribution of the different pathways. We will use an animal model to study the importance of middle-ear inertia and external-ear compression in bone conduction. The animal model allows us to measure physiological as well as acoustical and mechanical responses of the cochlea to both air- and bone-conduction stimulation. We will quantify the frequency range and significance of middle-ear inertia and ear canal compression to bone-conducted sound by comparing measurements of sound conduction made before and after interruption

of the middle-ear ossicular system. We hypothesize that cutting the middle-ear chain uncouples the two pathways that depend on relative motions of the ossicles and the inner ear: ear-canal compression and ossicular inertia. There are two specific aims to this thesis project.

1.5.1 Specific Aim 1: Determine the Relationship between Inner-Ear Sound Pressures and Physiological Cochlear Responses

We wish to validate our technique of differential intracochlear sound pressure (pressure in the scalae) measurement as an assessment of the cochlear mechanical response to bone vibration. To do so, we will test for proportionality between the differential intracochlear sound pressure measurements and a simultaneously measured cochlear sensory potential, the cochlear microphonic, a measure of the sensory output of the hair cells. Dancer and Franke [11] and Lynch et al. [12] demonstrated that in air conduction differential intracochlear sound pressure is proportional to cochlear microphonic potentials. This observation of proportionality is consistent with the notion that the differential intracochlear sound pressure is the drive for basilar membrane motion and the subsequent activation of the sensory hair cells within the cochlear partition. Measurement of the differential intracochlear sound pressure involves simultaneously monitoring the outputs of two ultra-small (less than 150 micrometers in diameter) fiber-optic pressure sensors, positioned on either side of the base of the cochlear partition. The difference in pressure at the base of the cochlear partition is also thought to be the common final stimulus to the inner ear for all of the bone-conduction paths and we hypothesize, as in air conduction, we would be able to see proportionality between the measured pressure difference and the cochlear microphonic. However, different bone-conduction mechanisms produce this pressure difference in different manners. For example, ear canal compression and middle-ear inertia produce a pressure at the oval window that is conducted to the round window in a manner similar to that of air conduction, with the result that the pressure

at the round window is consistently smaller than the pressure at the oval window [13]. Compressional bone conduction; however, simultaneously stimulates the entire cochlea and we expect the pressures at the windows to be related to the difference in the impedance at the windows. Therefore, measurements of the sound pressure on either side of the cochlear partition, together with their difference can help separate out the different BC pathways.

1.5.2 Specific Aim 2: Quantify the Contribution of the BC Stimulus Components that Depend on Ossicular Motion by Interruption of the Incudo-Stapedial Joint

Ear canal compression with the ear occluded and middle-ear inertia are considered by some to be major components in the conduction of bone conduction sound to the inner ear. We hypothesize that interrupting the incudo-stapedial joint will significantly reduce both of these components that depend on the relative motion of the ossicular chain and the inner ear. Comparison of the intracochlear sound pressures and sound pressure difference before and after this interruption will allow quantification of the sound pressure components that arrives at the inner ear via these pathways through calculation of the change in these pressures. Changes in the bone-conduction induced pressure difference that results from the interruption will also be compared to changes in the measured sensory potential to further evaluate the hypothesis that the pressure difference is the stimulus to the sensory apparatus.

Chapter 2

Material and Methods

We use chinchillas as an animal model to study the mechanisms of bone conduction and the relative significance of ossicular motion in bone conduction. Chinchillas were chosen because of their large middle-ear airspaces that allow easy access to the middle and inner ear for measurements and manipulation. In addition, our laboratory has much experience with this preparation.

Our approach is different from past experimental studies of bone conduction: we employed mechanical measurements together with physiological measurements while manipulating the structures of the middle ear. Stenfelt and coworkers [8] [14] used only mechanical measurements in cadaveric humans, while Tonndorf [25] used only physiological measurements that allowed estimation of the size of different stimulus components but did not provide adequate measurements of mechanism. Another difference in approach is our use of a Bone Anchored Hearing Aid (Cochlear BAHA) implanted on the animal skull as a vibrator. This device permits better stimulus control and reproducibility between animals. Stenfelt used a shaker that vibrates the whole cadaveric temporal bone in one particular direction favoring one mode of vibration over the others. We believe a vibration source applied to the whole skull will stimulate all of the potential stimulus modes that exist in clinical bone conduction.

In this chapter, we describe measurement tools and techniques necessary to our experiments.

2.1 Fiber-Optic Pressure Sensors

With their small size (150 μm diameter), high sensitivity (2.8 mV/Pa) and broad frequency bandwidth (100 Hz to 50 kHz), the in-house built fiber-optic pressure sensors provided adequate measurements of the pressure in the cochlea (scala vestibuli and scala tympani). The need for such a small size hydrophone is driven by the limited space and delicacy of the chinchilla cochlea [15]. The fiber-optic pressure sensors were designed, fabricated and calibrated as described by Olson [16]. There are three stages to the process:

1. Construction of the sensor tip and reflective gold-coated diaphragms
2. Assembly of the fiber-optic pressure sensor probes
3. Calibration of the probes to test its sensitivity and stability

2.1.1 Sensor Tip with Gold-Coated Diaphragm Construction

The sensor tips are composed of a 1-2 cm long hollow core glass capillary tube that is closed at one end by a gold-coated diaphragm. The diaphragm is made from a UV-cured thin film polymer approximately 0.5 μm in thickness. A tiny drop of Norland Optical Adhesive 68 (NOA68) is placed on a still surface of deionized water, cured by exposure to UV light. The cured adhesive film is affixed to one end of the capillary tube. The outer surface of the diaphragm is coated with a thin (450-500 μm) film of gold. The gold deposition is carried out at the Microsystem Technology Laboratories at MIT with its electron-beam evaporator, a high vacuum chamber capable of thin-film deposition through vaporization of the depositing materials. The addition of the gold makes the diaphragm highly reflective.

2.1.2 Fiber-Optic Pressure Sensor Probe Assembly

A single fiber optic (outer diameter of 120 μm) is inserted into the open end of the sensor tip till there is about a 50 μm gap between the fiber end and the inner surface

of the gold diaphragm. The fiber and the glass capillary tube are then glued together with UV-cured Norland adhesive. The optical fiber is spliced to a ‘Y’ coupling. One branch of the coupler is attached to a light-emitting diode (LED) that produces incoherent light, and the other branch is attached to a photodiode that measures the light reflected from the diaphragm (Fig. 2-1). The diaphragm flexes in response to sound and modulates the light reflected back down the fiber.

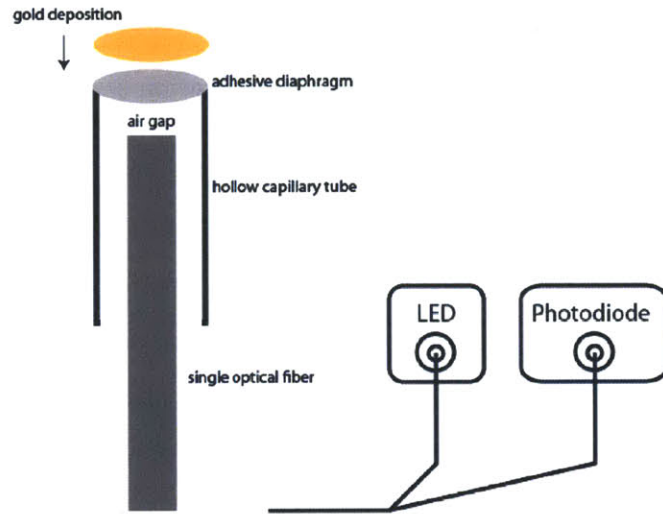


Figure 2-1: Schematic of the fiber-optic pressure sensor assembly.

2.1.3 Calibration: A Test of Sensitivity and Stability

The completed fiber-optic miniature microphone is calibrated in a vibrating water column using the method described by Schloss and Strasberg (1962) [17]. The pressure sensor is immersed in a vibrating column of liquid sitting on a shaker head and accelerometer (Brüel and Kjær 429) (Fig. 2-2). The pressure at the diaphragm is related to acceleration of the shaker a and immersion depth h given by Equation 2.1 where ρ is the density of the water.

$$P = \rho h a \quad (2.1)$$

Unfortunately, the sensors are fragile and prone to sensitivity change, thus careful handling is necessary. During the experiment, calibration of the sensor sensitivity is

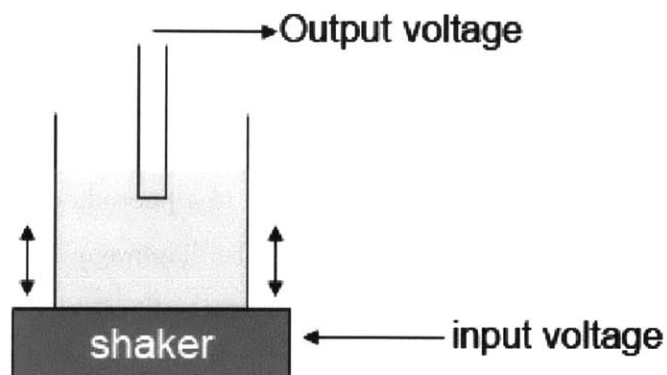


Figure 2-2: Schematic of a calibration setup.

performed repeatedly before and after each series of measurements to ensure that the sensitivity does not change significantly. Preliminary tests of the stability are also performed via repeated calibrations. Only measurements from stable sensors are used in our data analysis and reported here. The frequency dependence and sensitivity of a representative sensor are plotted in Figure 2-3. The solid and dashed curves represent the sensitivity of the sensor before and after the experiment. The frequency response of the sensor is generally flat up to 10 kHz. A stable sensor is defined as one in which the sensitivity changes by less than 3 dB.

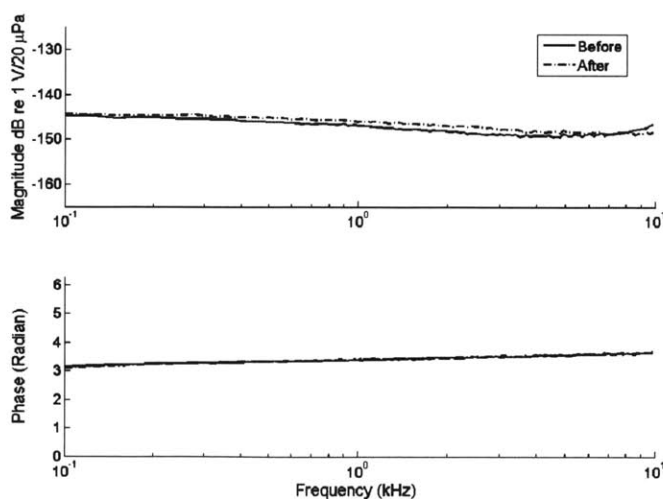


Figure 2-3: Frequency dependence and sensitivity of a representative sensor before and after an experiment.

2.2 Cochlear Potentials

A simple output of the sensory cells in the inner ear is the cochlear potential (CP), which also assesses the physiological condition and health of the sensory receptors. CP is the integrated vectorial sum of the electrical potentials generated by many hair cells, each excited at different amplitudes and phases [19]. It is recorded by placing an active electrode near the round window and a ground electrode in a neck muscle. It has been shown that when appropriate techniques are used, inferences can be drawn from CP to preceding mechanical responses [18], [19], [11]. We hope to test the relationship between CP and our measurements of differential intracochlear sound pressure at the base of the cochlea.

2.3 Animal Preparation

All animal procedures are approved by the Animal Care and Use Committee of the Massachusetts Eye and Ear Infirmary and MIT. The animals were anesthetized with Pentobarbital (50 mg/kg) and Ketamine (40 mg/kg), and their tracheas cannulated. The superior and posterior middle-ear cavities were opened. The tendon of the tensor tympani muscle was cut and the tympanic-portion of the VIIth nerve was sectioned to immobilize the stapedius muscle to prevent random contraction that can affect results [20]. The bony wall lateral and posterior to the round window (RW) was removed to visualize the surface of the round window and stapes footplate. The external ear was left intact, but a probe-tube microphone was inserted and sealed in place in the lateral end of the intact cartilaginous and bony ear canal near the tympanic membrane to measure ear canal sound pressure P_{EC} within 1 to 2 mm of the umbo of the malleus (Fig. 2-4). A cochlear potential CP electrode used for physiological measurement was implanted in the base of the cochlea below the round window membrane. To measure scala vestibuli pressure P_{SV} , a small hole (less than 250 μm in diameter) was made in the vestibule adjacent to the utricle after removal and retraction of a portion of the cerebellum posterior and medial to the vestibule. A second hole made in the cochlear

base near the round window was used to place the scala tympani pressure sensor P_{ST} . Both P_{SV} and P_{ST} measurements were made with our in-house built micro-optical pressure sensors.

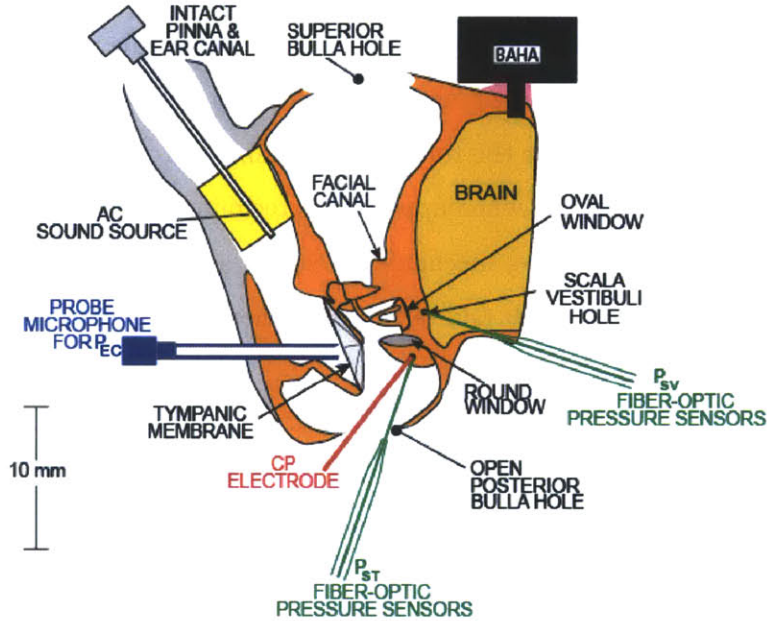


Figure 2-4: Schematic of the animal preparation and experimental setup.

2.4 Acoustic and Vibration Stimuli

Air conducted sound was delivered to the ear canal via an ER3A insert earphone (Etymotic) while bone conduction stimulation was delivered by a BAHA, Bone-Anchored Hearing Aid (Cochlea BAHA BP100) sound processor attached to a titanium screw implanted on the animal skull near the vertex. The use of the BAHA stimulator allowed us to move the animal head during experiment without affecting the reproducibility of our stimuli. The frequency response of the BAHA is bandpass in shape from 100 Hz to 8 kHz where the maximum peak is around 800 Hz. Since the chinchilla skull is thin, the standard 3 mm titanium screw was inserted only 1 mm deep into the skull and dental cement was used as a foundation and space filler to hold the screw in place. The BAHA was in its ‘direct audio input’ mode where electrical stimuli

are presented directly to the vibration processor and the microphone input to the processor is muted. The BAHA was programmed for ‘linear’ operation over the range of stimulus levels we used. The stimulus voltage input to either the ER3A or the BAHA are generated via a National Instruments I/O board controlled by a custom-built LabView program. A TDT-programmable attenuator was used to control the stimulus levels. The measurement protocol called for simultaneous measurements of P_{EC} , CP , P_{SV} , and P_{ST} during repeated presentations of stepped pure tones of 100 Hz to 10 kHz at 24 points/octave.

2.5 Experimental Procedure

Measurements of P_{EC} , CP , P_{SV} , and P_{ST} were made with tone sequences in both air conduction and bone conduction before and after manipulation of the middle ear. Measurements made at a variety of stimulus levels (over a 20 dB range) were consistent with linear responses. Once we established a good series of stable CP and pressure sensor measurements in the normal condition with an intact ossicular chain, we manipulated the middle ear using a tendon knife to interrupt the incudo-stapedial joint (IS-joint). After the interruption, measurements of P_{EC} , CP , P_{SV} , and P_{ST} were repeated in both AC and BC. The animal remained anesthetized throughout the whole procedure and was euthanized after completion of the experiment.

Chapter 3

Results

A total of 15 animals were used in this project: 9 ears with simultaneous measurements of CP and intracochlear sound pressures, P_{SV} and P_{ST} ; 4 ears with only CP measurements and 2 ears without any measurements due to complications in our surgical preparation.

We measured both cochlear potential CP and inner ear sound pressures evoked by AC and BC. The cochlear potential (CP) measured at the round window is a weighted sum of the sound-evoked sensory and neural potentials within the inner ear. At low and moderate stimulus levels, the CP grows linearly; however, it saturates with high stimulus levels [29]. In our experiments, we measured the CP at different stimulus levels to define a level range where the response was linear. Figure 3-1 shows measurements of the magnitude of the CP evoked by different AC and BC stimulus levels (so-called input-output curves) at different frequencies in one experiment. The magnitude of the CP generally grew linearly with stimulus level (the black dashed line indicates a 1 dB/dB input-output relationship).

Calibrations of the pressure sensors were performed before and after each set of P_{SV} and P_{ST} measurements in order to check the sensitivity and stability of the sensor probes. For the most part, the data reported in this thesis work only includes those measurements in which the sensitivity of the sensor varied by less than 3 dB. In a few cases; however, sensitivity of the post measurement calibration was used to describe the sensor during measurements based on the reasoning that the sensor

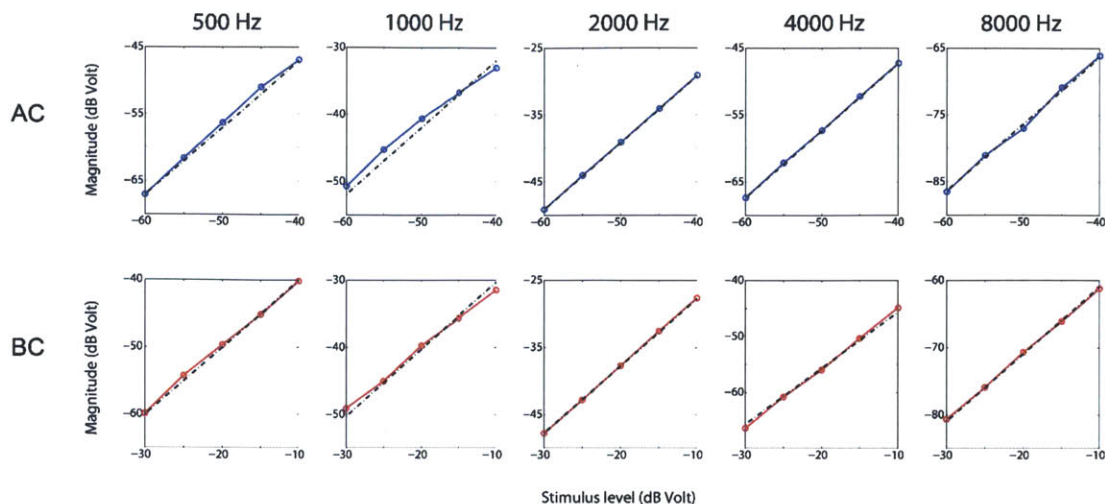


Figure 3-1: Magnitude of CP response curves evoked by AC and BC at different frequencies in one experiment. The abscissa describes the voltage input to the AC and BC transducer in terms of dB re 1 volt. Linear growth of CP was generally observed with AC sound stimuli of less than 80 dB SPL, and BC vibratory stimuli of less than 35 dB mm/s^2 .

probe was less prone to traumatization when pulled out compared to when it is inserted. In addition, only data gathered with a signal-to-noise ratio of 10 dB or higher are included in the analysis (signal to noise was estimated by observation of the magnitude of off-stimulus frequency components determined when we computed Fourier transforms of the responses to sinusoidal stimulation). For comparison with other measurements taken in different ears, our AC data were normalized by ear canal sound pressure P_{EC} . BC data were normalized by the voltage used to drive the BAHA.

3.1 Inner-Ear Responses to Air Conduction and Bone Conduction: ΔP and CP

In analyzing normal inner-ear responses to AC and BC, we included only the 9 ears in which we measured both CP and the inner-ear sound pressures.

3.1.1 Intracochlear Sound Pressure Measurements in AC

Figure 3-2 shows frequency response measurements of the CP and intracochlear sound pressures measured in 9 ears with AC stimulation. Their means and standard deviation are also included. The magnitude of P_{SV} , P_{ST} , CP and ΔP are shown in panel A, B, C, D respectively. For frequencies below 2 kHz, scala vestibuli sound pressure P_{SV} is 10 to 20 dB higher than scala tympani sound pressure P_{ST} (comparing the mean data in panel A and B of Fig. 3-2). This difference in level is also evident in Figure 3-3 where we plot the ratio of P_{ST} over P_{SV} in the individual animals, as well as the mean and standard deviation.

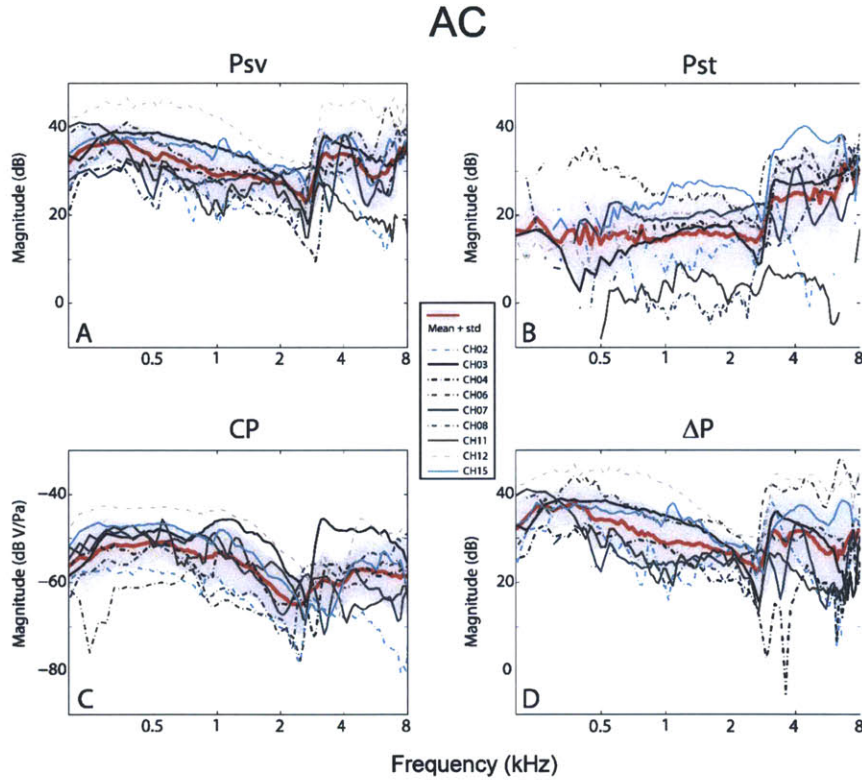


Figure 3-2: Normalized P_{SV} , P_{ST} , CP and ΔP in AC in nine individual animals. The red lines illustrate the means and gray-shaded area illustrates ± 1 standard deviation around the mean. All measurements are normalized by the sound pressure in the ear canal; panels A, B & D plot a dimensionless ratio of two pressures, and panel C plots a dB representation of the ratio of V/Pa.

As frequency increases, the two pressures become more similar in magnitude. However, throughout the measurement frequency range, the magnitude of P_{SV} was generally larger than that of P_{ST} . The differential intracochlear sound pressure ΔP was computed as the vector difference between P_{SV} and P_{ST} . In AC, ΔP (Fig. 3-2 D) is similar to P_{SV} (Fig. 3-2 A) because P_{SV} is significantly larger than P_{ST} over all but the highest stimulus frequencies. The frequency dependences of CP (Fig. 3-2 C) and ΔP (Fig. 3-2 D) are similar. A direct comparison of the two is made in a later section.

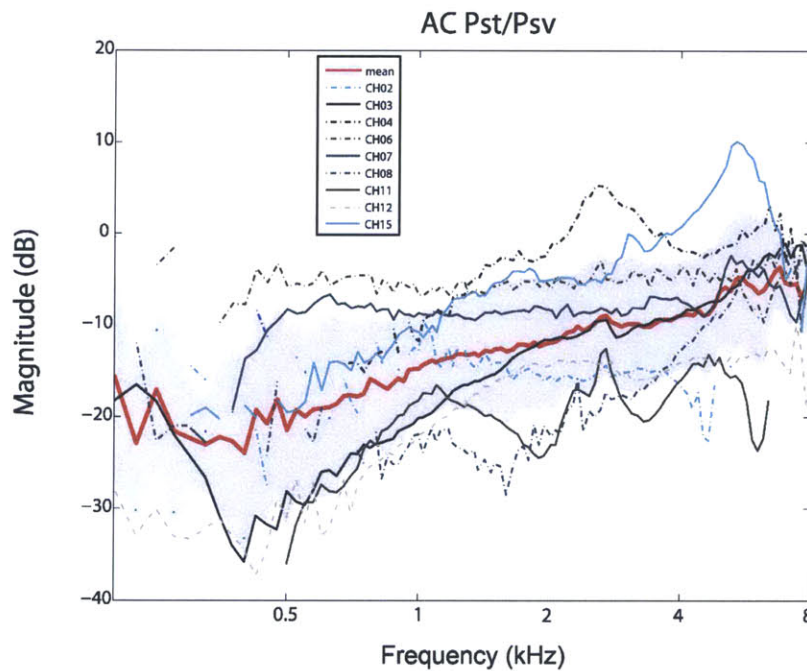


Figure 3-3: Ratio of P_{ST} over P_{SV} in AC in the nine individual animals. The red line illustrates the mean and the gray-shaded area illustrates ± 1 standard deviation around the mean.

3.1.2 Intracochlear Sound Pressure Measurements in BC

Figure 3-4 shows P_{SV} , P_{ST} , CP and ΔP in response to BC stimulation. In bone conduction, P_{SV} and P_{ST} are more similar in magnitude: P_{SV} is generally only 10 dB greater than P_{ST} (Fig. 3-5). The frequency dependence of the two pressures normalized by stimulus voltage are parallel but converge at higher frequencies, as

they do in AC. As in AC, the differential intracochlear sound pressure ΔP is nearly identical to P_{SV} since the magnitude of P_{SV} is larger than P_{ST} at most frequencies except at 4 kHz. The drop-off in P_{SV} , P_{ST} and CP magnitudes at high frequency results from a decrease in the output of the BAHA (Fig. 3-6).

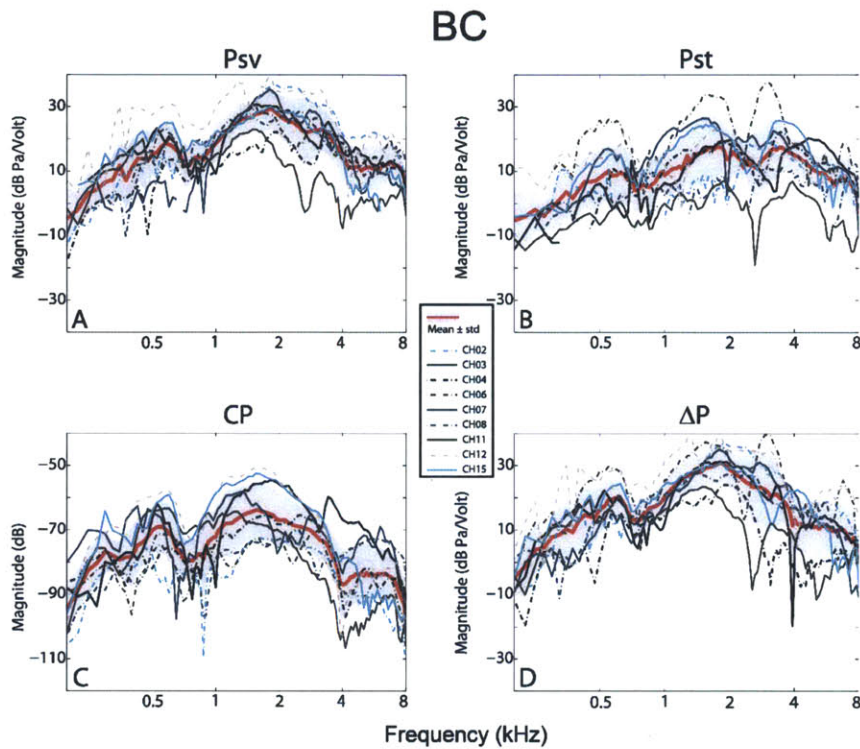


Figure 3-4: P_{SV} , P_{ST} , CP and ΔP in BC in nine individual animals. The red lines illustrate the means and the gray areas ± 1 standard deviation around the mean. All panels represent the ratio of the measured pressure or CP and the voltage drive to the BC stimulator.

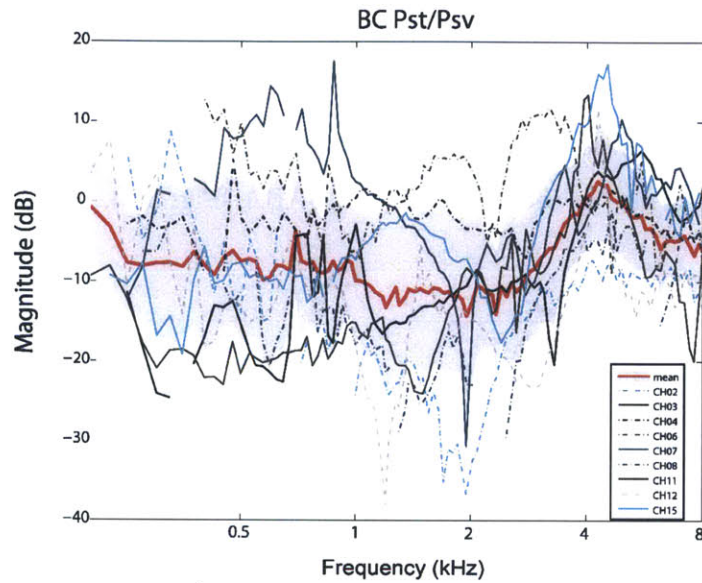


Figure 3-5: Ratio of P_{ST} over P_{SV} in BC in the nine individual animals. The red line illustrates the mean and the gray-shaded area illustrates ± 1 standard deviation around the mean.

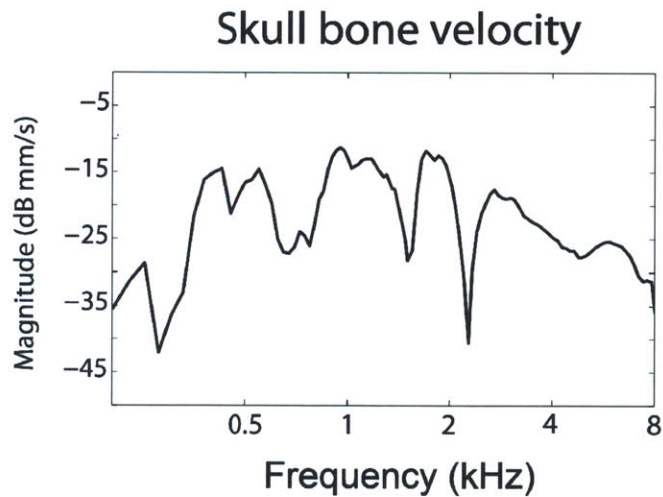


Figure 3-6: A measure of the velocity of the skull evoked by the BC stimulus in one experiment. The velocity was measured with a one-dimensional laser Doppler vibrometer. The vibrometer was positioned to be sensitive to a combination of lateral and up and down skull motions. The magnitude of the velocity falls off below 0.4 kHz and above 4 kHz.

3.1.3 Comparison of CP and ΔP in AC and BC

A basic tenant of our analysis is that the difference in sound pressures on either side of the cochlear partition ΔP is the fundamental stimulus that excites the cochlear traveling wave which triggers the sensory response to sound and vibration. We wish to test this hypothesis by comparing the frequency dependence of our inner-ear sound pressure and cochlear potential measurements during both AC and BC stimulation.

One of the challenges in our experiments was to maintain a healthy CP throughout the experiments while being able to measure intracochlear sound pressure. In general, the CP level was adversely affected by our opening of holes into the inner ear and placing our pressure transducers. This instability of the CP made it hard to compare directly simultaneous measurements of the CP and ΔP . Instead we compare in Figures 3-7 and 3-8 CP measurements made prior to making the holes and placing the pressure transducers in the ear with ΔP , which by necessity was measured after placement of the pressure sensors.

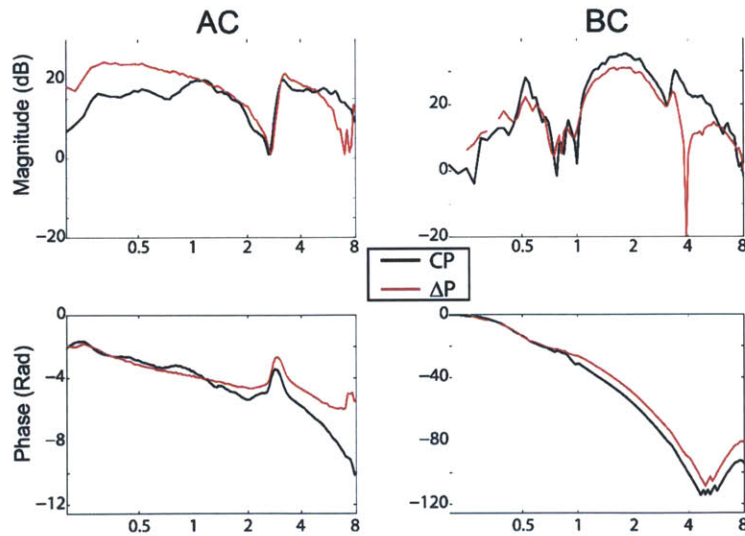


Figure 3-7: Cochlear potential CP and differential intracochlear sound pressure ΔP measurements in AC and BC in ear CH03. The CP data have been scaled to match the pressure data.

A demonstration of correlation between CP and ΔP would support our use of differential intracochlear sound pressure measurements to investigate inner-ear responses to AC and BC. Figure 3-7 shows the magnitude and phase of CP and ΔP in a single ear during both AC and BC stimulation. While the CP and ΔP do not strictly overlap, their overall frequency dependence and the fine structures of their magnitude and phase response show clear similarities during both AC and BC stimulation. Figure 3-8 shows similar comparisons of the measured magnitudes for all 9 ears in which we have both pre-sensor CP measurements and ΔP .

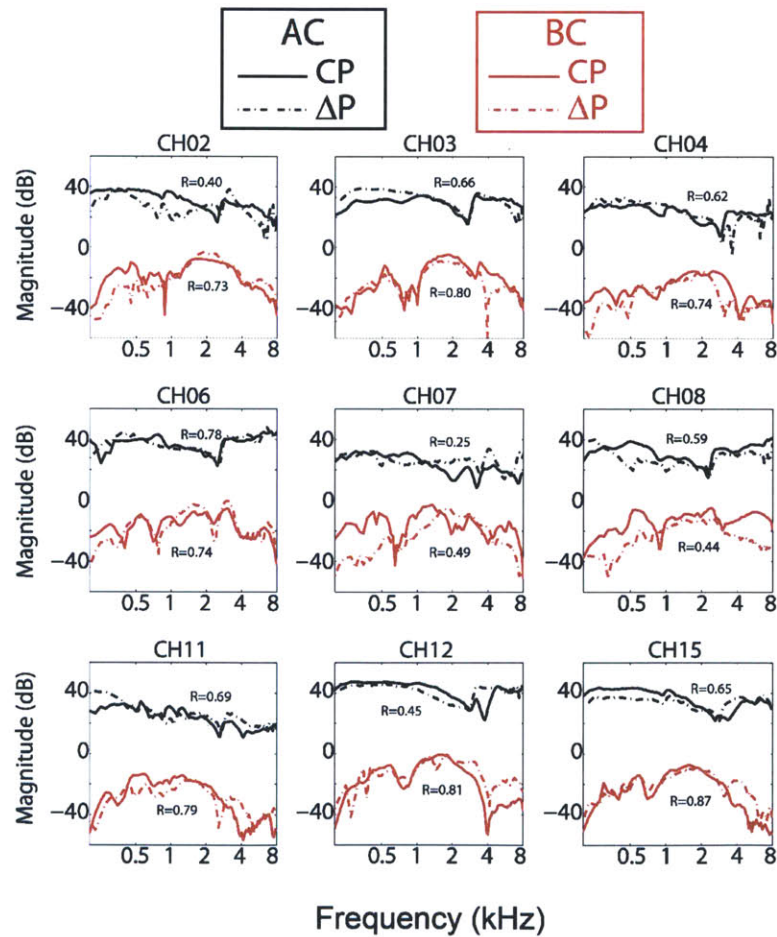


Figure 3-8: Comparison of magnitude of cochlear potential CP and differential intracochlear sound pressure ΔP in AC and BC in nine ears. The CP data have been scaled to best match the pressure data. The R values are discussed below.

We used a correlation analysis to quantify the match between CP and ΔP in AC and BC. The correlation coefficient is a measure of the strength of linear dependence between the two variables. Using a MATLAB routine called ‘corr’, we computed in logarithmic scale the correlation coefficient of the magnitude of CP and ΔP measurements made with AC and BC in each of the 9 ears. The formula of R is given by Equation 3.1. The square of R is the fraction of the variance in y that is explained by variation in x .

$$R(x, y) = \frac{\sum_{i=1}^n x_i y_i - \frac{\sum_{i=1}^n x_i \sum_{i=1}^n y_i}{n}}{\left(\sum_{i=1}^n y_i^2 - \frac{(\sum_{i=1}^n y_i)^2}{n} \right) \left(\sum_{i=1}^n x_i^2 - \frac{(\sum_{i=1}^n x_i)^2}{n} \right)} \quad (3.1)$$

Table 3.1 shows R values, the correlation coefficient, in both AC and BC stimulation. The closer the R is to 1, the stronger the correlation between the CP and ΔP and the stronger the proportional relationship. An R of 0.5 in AC was chosen as the threshold (highlighted in yellow in Table 3.1) for defining ‘reasonable’ proportionality between CP and ΔP (Fig. 3-8), where this value corresponds to at least 25% of the variance in CP being explained by the variation in ΔP . This level of match was obtained in 6 of the 9 AC measurements and 8 of the 9 BC measurements. Five of the 9 ears achieved this level of correlation in both AC and BC testing. In 7 of the 9 BC measurements R was better than 0.71, consistent with at least 50% of the variance in CP being explained by variation in ΔP .

Table 3.1: Correlation coefficient in AC and BC

Chinchilla number	R_{AC}	R_{BC}
2	0.40	0.73
3	0.66	0.80
4	0.62	0.74
6	0.78	0.74
7	0.25	0.49
8	0.59	0.44
11	0.69	0.79
12	0.45	0.81
15	0.65	0.87

Even though we see differences in the specifics of the frequency responses of CP and ΔP in both AC and BC, Figures 3-7, 3-8, and Table 3.1 support an overall proportionality of these responses.

3.2 Effects of Middle-Ear Ossicular Chain Interruption in AC and BC

Out of 15 animals, successful and complete interruption of the incudo-stapedial joint (IS-joint) was achieved in 12 ears. Eight of which had both CP and intracochlear sound pressure (P_{SV} and P_{ST}) measurements while 4 had only CP measurements. Figure 3-9 shows P_{SV} , P_{ST} , CP , and ΔP with AC and BC stimulation from one experiment before and after the incudo-stapedial joint interruption. After the interruption, measurements of inner ear responses with AC stimulation drops by as much as 40 dB (black curves of Fig. 3-9; interrupted data is shown as dashed lines). While effects of ossicular joint interruption on inner ear responses in AC stimulation are significantly large, in BC the effects of interruption are relative small, at most 15 dB (red curves of Fig. 3-9). The largest drop is seen on P_{SV} after the interruption. There is little change to P_{ST} and small change to ΔP . Close inspection of the data in Figure 3-9 points out that some of the data points are missing. This is the result of our 10 dB of signal-to-noise ratio filtering; missing points did not pass the 10 dB signal-to-noise test. Because the measured values after IS-joint interruption are smaller, especially in AC stimulation, a majority of the missing points data are from post-interruption measurements.

The observation of large interruption-induced changes in AC, and smaller changes in BC is generalized to all measurement ears in Figures 3-10 and 3-11 where the data from all ears are plotted along with the mean and standard deviation. The different panels in Figures 3-10 and 3-11 illustrate the changes, denoted by Δ , produced by the interruption on inner ear pressures (ΔP_{SV} , ΔP_{ST} , and $\Delta(\Delta P)$) as well as the CP (ΔCP).

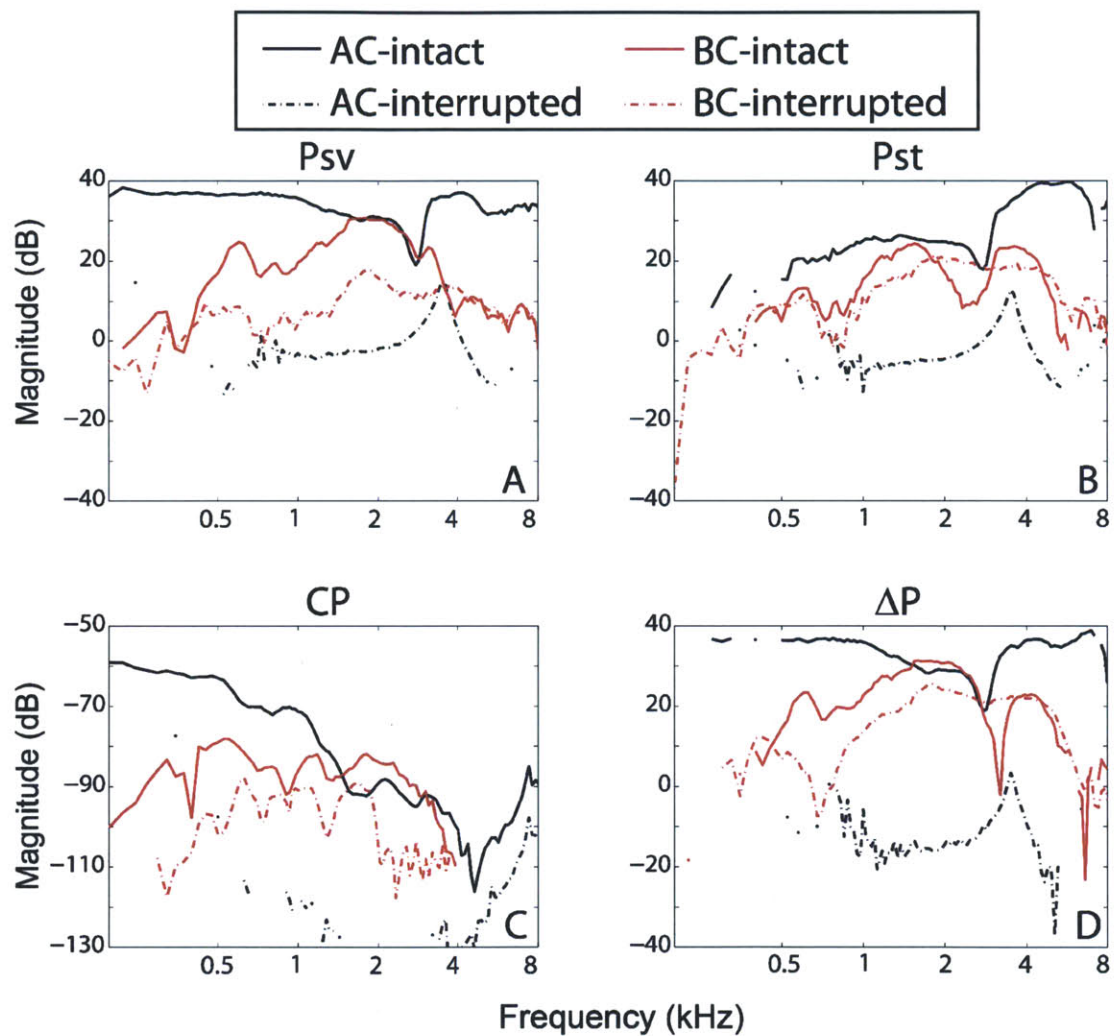


Figure 3-9: Inner ear responses P_{SV} , P_{ST} , CP , and ΔP in AC and BC before and after IS-joint interruption from one experiment (Ear CH15).

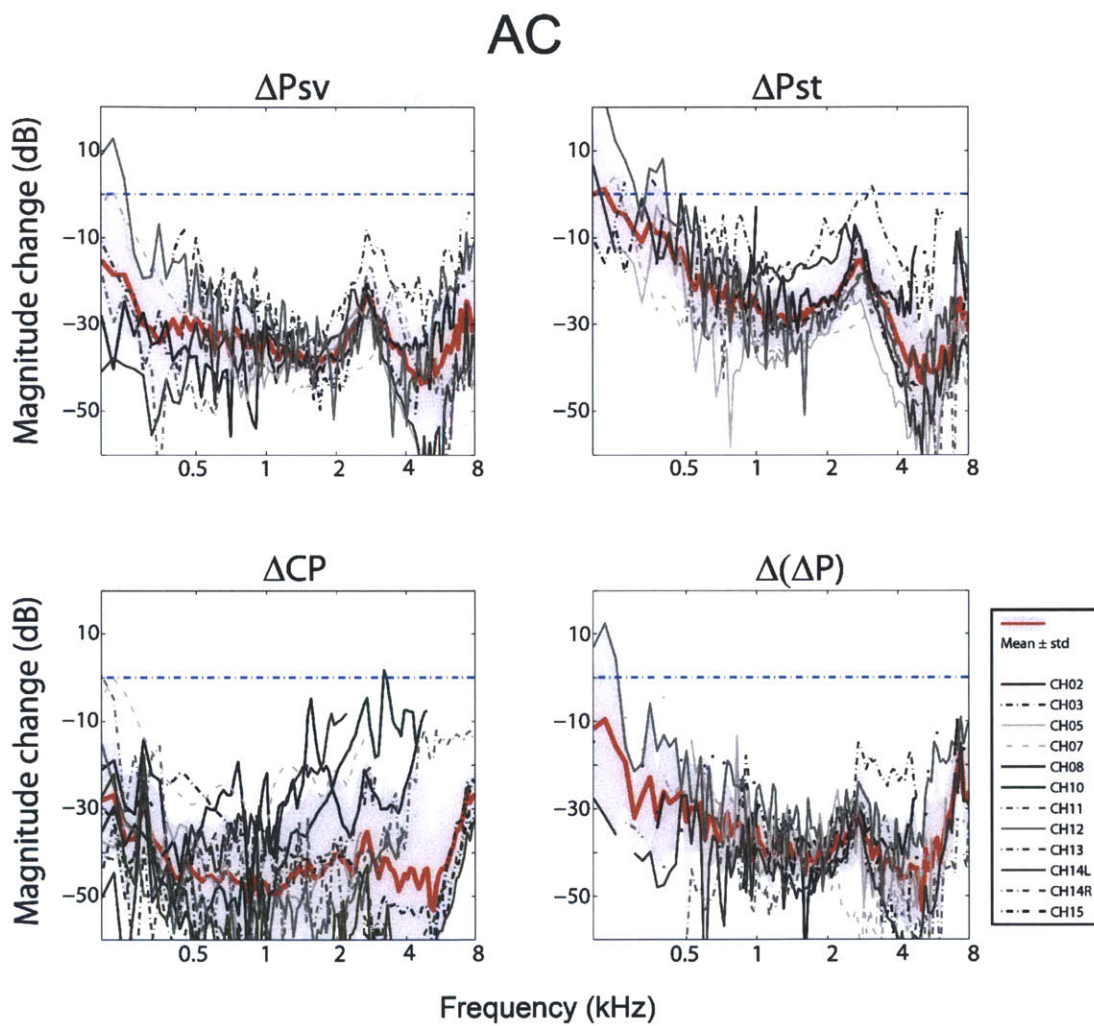


Figure 3-10: Effects of incudo-stapedial joint interruption in AC on P_{SV} , P_{ST} and ΔP for 8 ears and CP for 12 ears including the mean and standard deviation.

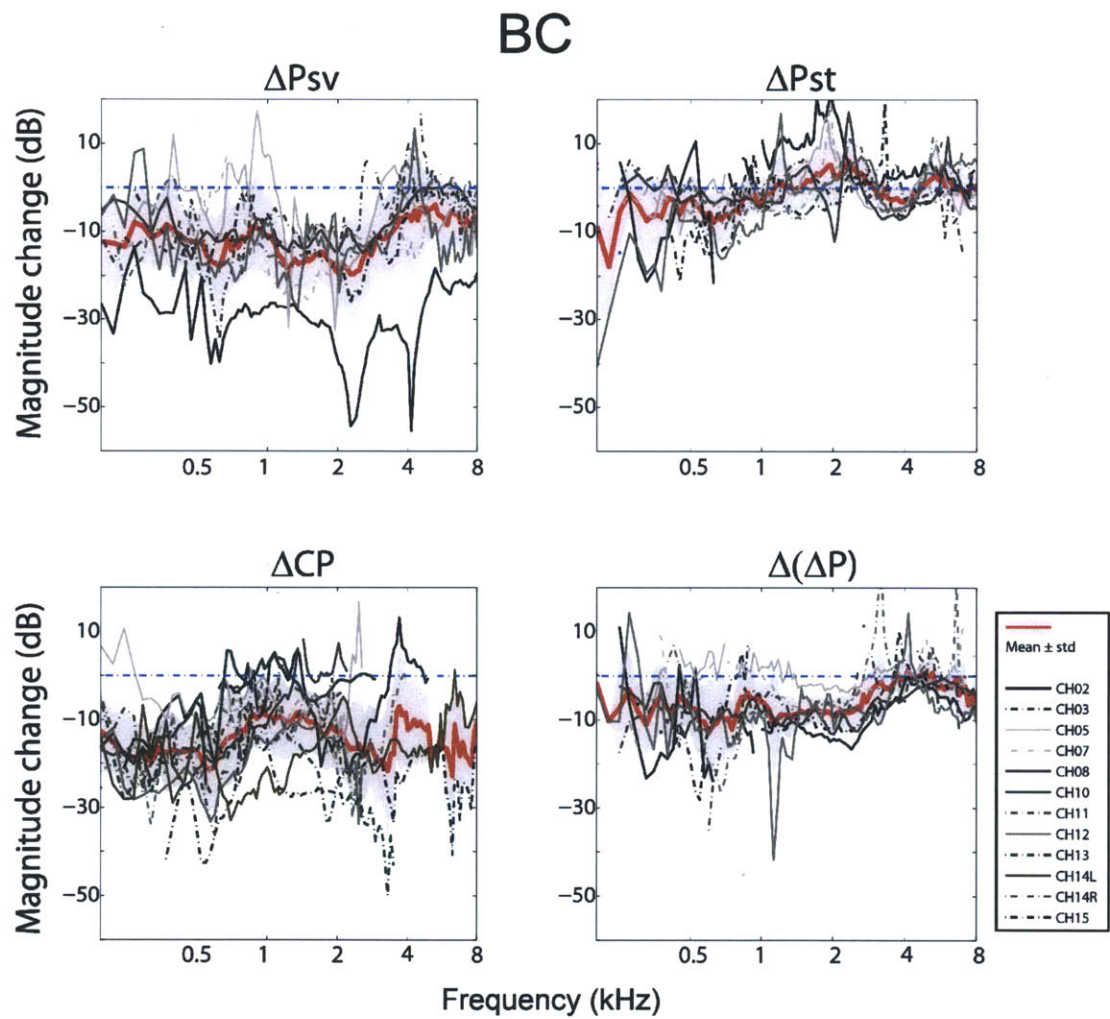


Figure 3-11: Effects of incudo-stapedial joint interruption in BC on P_{SV} , P_{ST} and ΔP for 8 ears and CP for 12 ears including the mean and standard deviation.

Chapter 4

Discussion

4.1 Is the Differential Intracochlear Sound Pressure the Driving Source to the Sensory Response of the Inner Ear in AC and BC?

Our comparison of the CP and ΔP in individual ears suggests the differential intracochlear sound pressure ΔP , which is the mechanical input to the cochlea, and the sensory response CP , which is the electrical output of the sensory organ (organ of corti), are proportional as noted by correlation coefficients computed from the magnitude of CP and ΔP (Fig. 3-8). The finding in AC is consistent with the demonstration by Dancer and Franke [11] and Lynch et al. [12] that differential intracochlear sound pressure measurement and cochlear microphonic potentials measured in guinea pigs and cats were proportional. This observed proportionality is consistent with the hypothesis that the differential intracochlear sound pressure is the driving force to basilar membrane motion, the cochlear traveling wave and subsequent activation of the sensory organ. In BC, our observation of proportionality between CP and ΔP is consistent with the mechanical stimulus to the inner ear being the same as in AC. This finding is in line with two observations. 1). Békésy experimentally demonstrated that pure tones stimulated by bone vibrator can be subjectively cancelled by pure tones of AC [22] indicating that basilar membrane motion is excited the same way in

both AC and BC. The study of AC and BC pure-tone cancellation was later extended by Stenfelt [26] among others. 2). Measurements of basilar membrane motion show similar patterns of excitation independent of whether the stimulus is AC or BC [27].

4.2 Evidence for the Contribution of Multiple Mechanisms to the BC response in the Normal Measurements

While there is much data supporting the hypothesis that the final acousto-mechanical response produced by BC is a trans-cochlear pressure difference that evokes cochlear traveling wave as in AC, how the multiple pathways of BC combine to induce this inner-ear response has not been determined. In air conduction, where the stimulus path includes relative motion of the stapes and the cochlea, we expect pressure at the oval window to be significantly larger than pressure at the round window, where the inner ear is bounded by a highly compliant membrane [32]. This is evident in our data (Fig. 3-2) where P_{SV} is generally 20 dB larger than P_{ST} at the lowest frequencies and the difference decreases as frequencies increase. The ratio of P_{ST} over P_{SV} has a positive slope of 0.5 (see Fig. 3-3). In bone conduction, our mean data (Fig. 3-4) show $|P_{SV}|$ larger than $|P_{ST}|$ by only 10 dB below 4 kHz. At 4 kHz, the two pressures were of similar magnitude and at higher frequencies $|P_{SV}|$ is again larger than $|P_{ST}|$. The ratio of P_{ST} over P_{SV} is independent of frequency below 4 kHz which differs from that in the AC case.

The differences between the behavior of P_{ST} and P_{SV} in AC and BC tell us something about the significance of different BC sound paths. If either the outer ear or middle ear pathways play a dominant role in producing the intracochlear sound pressure in BC, we would expect similarities in the ratio of and differences between the two intracochlear sound pressures P_{SV} and P_{ST} in AC and BC. This is because BC outer ear compression (the occlusion effect) and middle ear inertia act on the inner ear by way of inducing relative motion between the ossicles and the cochlea.

Thus, their contribution in BC process should produce differences in intracochlear sound pressure similar to that of AC. That a nearly frequency-independent 10 dB difference is seen between the two pressures below 4 kHz, suggest that the resulting intracochlear sound pressures in BC are significantly affected by other BC pathways. Those pathways must originate within the inner ear or the skull and braincase. If this is the case, assuming volume velocity produced by BC inner-ear pathways at the two windows are of the same magnitude, we would expect the pressure near the two windows to be related to the window impedances ($P = U \times Z$ where U is the volume velocity and Z is the impedance). Ravicz et al. [33] estimated the impedance seen from the cochlea looking out through the oval window in chinchilla to be 100 G Ω at 1 kHz, while a model of Ravicz et al. [13] suggests the impedance at the round window is on the order of 10 G Ω at 1 kHz. These impedance estimates, together with the assumption of equal volume velocity magnitude at the two windows, predict that the pressures at the two windows will differ by an order of magnitude, which is equivalent to 20 dB, at 1 kHz. Our data shows P_{SV} is only 10 dB larger than P_{ST} in BC stimulation. From comparison of the inner ear sound pressures P_{SV} and P_{ST} in both AC and BC in the normal ears, it is suggested that no single BC mechanism offers a complete explanation to our data. It is most likely the combination of multiple pathways that contribute significantly to the BC process.

4.3 Evidence for the Contribution of Inner Ear Mechanisms to the BC response in the Measurements Made After Middle Ear Interruption

The effect of middle ear interruption on the different cochlear pressures also helps us quantify the relative importance of different BC pathways, which is one of the goals of this work. Ossicular chain interruption (cutting the IS-joint) causes significant

decreases in the inner ear response to AC stimulation. A decrease of as much as 40 dB can be seen in both ΔP and CP (Fig. 3-10). This is expected because the primary pathway for sound conduction to the inner ear has been interrupted. In BC, the interruption causes smaller changes. P_{SV} only drops by an average of 10 dB; P_{ST} is little affected; CP decreases by 15 dB; and the decrease in ΔP is similar to that of P_{SV} and CP .

In BC, the interruption of the IS-joint must significantly reduce the contribution of two pathways dependent on the ossicular transduction of sound to the inner ear: ear canal cartilaginous compression of the occluded ear canal (we had an AC sound source in place for the whole experimental period) and middle-ear inertia. The drop of 10 dB in P_{SV} can be explained by two mechanisms, or their combination. First, the drop may be related to the reduction of the contribution of outer-ear compression and/or middle-ear inertia with IS-joint interruption. Second, it may be related to the interaction of cochlear compressive or inertance mechanisms with the decreased impedance looking out of the oval window after IS-joint interruption.

If the first suggested mechanism is correct, we would expect to see similar effects on both P_{SV} and P_{ST} , where the decrease in $|P_{ST}|$ would be of the same magnitude as that of $|P_{SV}|$, as we observed in AC (Fig. 3-10). The observation of little change in P_{ST} after IS-joint interruption suggests ear canal and middle ear pathways are not significant in BC in this condition.

The second suggested mechanism is consistent with the observed changes in P_{SV} and P_{ST} . In this mechanism, the interruption not only reduces the sound conduction from outer ear or middle ear BC pathways, but also decreases the impedance seen looking from the cochlea out through the oval window. Pressure is proportional to the impedance, and a decrease in the oval-window impedance, which constrains the volume velocity at the oval window produced by inner ear sources, would lead to a decrease in $|P_{SV}|$. P_{ST} on the other hand would be little affected by this impedance change, since the impedance of the round window should be unchanged by IS-joint interruption. The predicted decrease in $|P_{SV}|$ with little change in $|P_{ST}|$ matches our results. Therefore, the post-interruption data clearly implies that BC inner ear

pathways play a significant role in producing the intracochlear sound pressure.

4.4 Comparison of Intracochlear Sound Pressure of the Current Study to Other Studies

The average intracochlear pressure measurements of P_{SV} , P_{ST} and ΔP and their standard deviation in air conduction of the current study were compared to those of Ravicz et al. [13] [30], Slama et al. [15], and Décory et al. [31] (Fig. 4-1). The magnitude of P_{SV} in the current study is about 10 dB greater than that of Ravicz et al. [30], 20 dB larger than Ravicz et al. [13], and comparable to the mean data of Slama et al. [15] and Décory et al. [31]. P_{ST} measurement was about 15 dB larger than that of Ravicz, but similar to that of Décory et al. The differential intracochlear sound pressure ΔP is similar to P_{SV} , thus the ΔP difference between the current study and Ravicz's is within 10 dB. Despite the large P_{ST} in the current study, it does not affect our calculation of the differential intracochlear sound pressure. ΔP is largely dominated by P_{SV} . The phase of the intracochlear sound pressure P_{SV} and P_{ST} is similar to that of the previous studies (bottom plots of Fig. 4-1).

The difference of P_{SV} measured in this study compared to Ravicz's is likely not due to a difference in method used to place the pressure sensor probe within scala vestibuli. We accessed the vestibule by retracting the cerebellum within the paraflocculus to expose the medial-superior wall of the vestibule. Ravicz's approach was from the posterior cavity. However, Slama et al. [15] measured P_{SV} with the same method as Ravicz et al. [13] [30] and our scala vestibuli sound pressure measurement P_{SV} is similar to Slama et al. [15].

P_{ST} measurement of the current study is 10 to 15 dB higher than Ravicz et al. [13] [30] even though measurement location is approximately the same: a hole for P_{ST} measurement is located at the base of the cochlea a few mm below the round window membrane. Our results are more similar to those of Decory et al. [31]. We know of no methodological differences that can explain the selective differences and

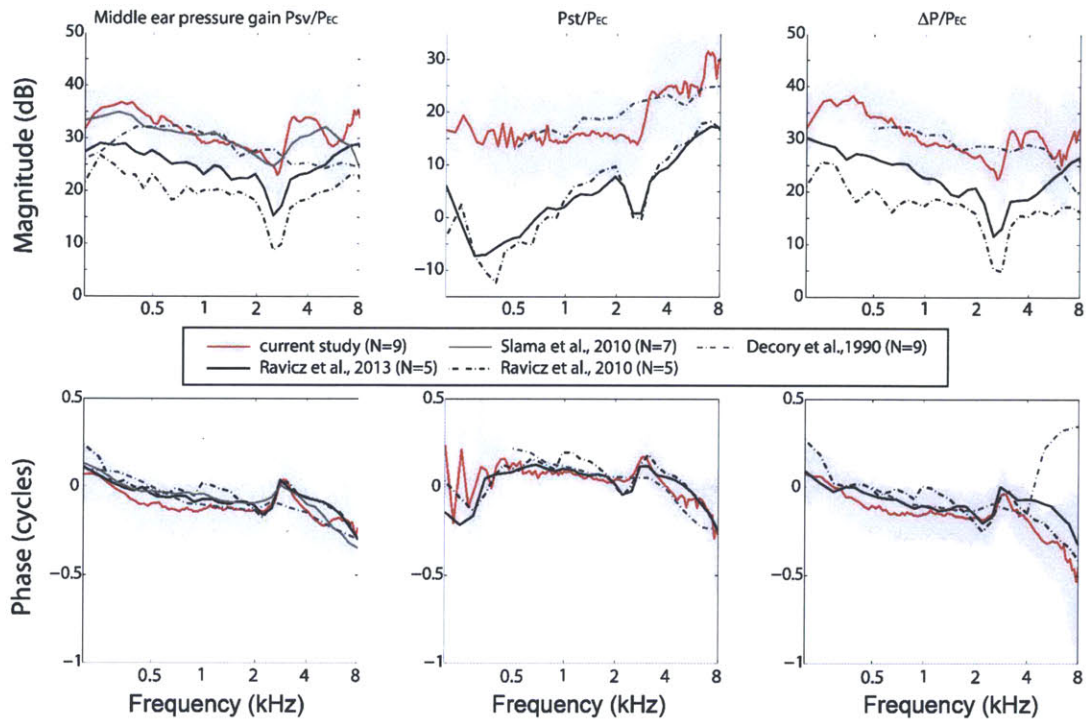


Figure 4-1: P_{SV} , P_{ST} , and ΔP in AC in comparison with previous studies.

similarities.

Chapter 5

Conclusions

This thesis work investigated the relative significance of two major components in bone conduction mechanisms: middle ear inertia and inner ear compression. Inner-ear sound pressure and cochlear potential were measured in 12 live anesthetized chinchillas before and after interruption of the incudo-stapedial joint. Following are the summary and interpretation of data obtained from this experimental work.

- We have demonstrated the use of in-house built miniature fiber-optic pressure transducers to simultaneously measure sound pressures in the cochlea: sound pressure in the scala vestibuli P_{SV} and scala tympani P_{ST} . The ability to obtain simultaneous measurements of the inner-ear sound pressure provides insights into how the inner ear is stimulated in bone conduction.
- We have measurements of the cochlear potential and inner-ear sound pressure within the same animal which allow us to quantify their relationship.
- We have shown a reasonable correlation between the mechanical drive, the differential intracochlear sound pressure ΔP , and the sensory output of the cochlear, the CP , in both AC and BC. The proportional behavior between the two allows us to use inner-ear sound pressures to compare and contrast possible pathways in BC to AC.
- In response to AC stimulation, P_{SV} is 20 dB larger than P_{ST} at low frequencies

and their difference decreases as frequencies increase. The ratio between P_{ST} and P_{SV} has a slope of 0.5.

- In response to BC stimulation, P_{SV} is only 10 dB larger than P_{ST} and their ratio is frequency independent below 4 kHz, which is different from that in the AC case.
- Comparison of the two intracochlear sound pressures P_{SV} and P_{ST} in AC and BC in the normal ears suggests no individual mechanism of BC is responsible for producing the inner-ear response. Instead, it is a collection of multiple pathways and their interaction that contributes to BC response.
- Data of inner ear response in AC and BC after middle-ear ossicular chain interruption provided evidence for the relative significance of the inner ear mechanisms in BC process.
- The data further suggest outer ear compression and middle ear inertia play a less important role compared to the inner ear pathways in BC response.

While this study provided insights into how bone conduction works, further investigation into different pathways of bone conduction is needed. Outer ear canal cartilaginous wall compression as well as the occlusion effect can be studied by observing the changes to inner ear responses while occluding and unoccluding the ear canal. Inner ear compression pathway can be further investigated by measuring inner ear responses with normal and fixed stapes.

Bibliography

- [1] Anthony F. Jahn and Joseph Santos-Sacchi. (2001). *Physiology of the ear*, 2nd Edition, Singular.
- [2] Rosowski JJ. Outer and middle ear. In: Fay RR, Popper AN, editors. *Comparative Hearing in Mammals*. Springer-Verlag; New York: 1994. pp. 172-247.
- [3] Ng M, Jackler R. (1993). Early history of tuning-fork tests, *Am J Otolaryngol* 1993; 14:100-105.
- [4] Goldstein, D., and Hayes, C. (1971). "The occlusion effect in bone-conduction hearing," in *Hearing Measurement: A Book of Readings*, edited by I. Ventry, J. Chaiklin, and R. Dixon (Appleton-Century-Crofts, New York), pp. 150-157.
- [5] Freeman S, Sichel JY, Sohmer H. Bone conduction experiments in animals - evidence for a non-osseous mechanism. *Hear Res.* 2000;146:72-80.
- [6] Stenfelt S, Goode RL: Bone conducted sound: Physiological and clinical aspects. *Otol Neurotol* 2005;26:1245-1261.
- [7] Stenfelt S. (2006). Middle ear ossicles motion at hearing thresholds with air conduction and bone conduction stimulation. *J Acoust Soc Am* 2006;119:2848-2858..
- [8] Stenfelt S, Hato N, Goode RL. (2002) Factors contributing to bone conduction: The middle ear. *J Acoust Soc Am* 2002;111:947-959.
- [9] Minor LB. (2000). Superior canal dehiscence syndrome, *Am J Otol.* 2000 Jan;21(1):9-19.
- [10] Songer, J.E., Rosowski, J.J. (2008). A mechano-acoustic model of the effect of superior canal dehiscence of hearing in chinchilla, *J. Acoust. Soc.Am.* 122(2):943-51.
- [11] Dancer A. and Franke R. (1980). Intracochlear sound pressure measurements in guinea pigs, *Hear. Res.* 2, 191-205.
- [12] Lynch, T. J. III, Nedzelnitsky, V., and Peake, W. T. (1982). Input impedance of the cochlear in cat, *J. Acoust. Soc. Am.* 72, 108-130.

- [13] Ravicz, ME, Slama, MC, Rosowski, JJ. (2010). Middle-ear pressure gain and cochlear partition differential pressure in chinchilla, *Hear Res.* 2010 May;263(1-2):16-25.
- [14] Stenfelt, S., Hato, N., and Goode, R., 2004, Fluid volume displacement at the oval and round windows with air and bone conduction stimulation, *J. Acoust. Soc. Am.* 115(2), 797-812. Also published in February 1, 2004 issue of *Virtual Journal of Biological Physics Research* (<http://www.vjbio.org>).
- [15] Slama, M.C.C., Ravicz M.E., Rosowski, J.J. (2010). Middle ear function and cochlear input impedance in chinchilla, *J. Acoust. Soc. Am.* 127 (3):1397-1410.
- [16] Olson, E.S. (1998). Observing middle and inner ear mechanics with novel intracochlear pressure sensors, *J. Acoust. Soc. Am.* 103: 3445 3463.
- [17] Schloss F. and Strasberg M. (1962). Hydrophone calibration in a vibrating column of liquid, *J. Acoust. Soc. Am.* 34(7):958-960.
- [18] Dallos, P. (1973). Cochlear potentials and cochlear mechanics in basic mechanisms of hearing, edited by A. Moller (Academic, New York) 335-376.
- [19] Dallos P, Cheatham MA, and Ferraro J. (1974). Cochlear mechanics, nonlinearities, and cochlear potentials, *J. Acoust. Soc. Am.* 55(3):597-605.
- [20] Rosowski, J.J., Ravicz, M.E., Songer, J.E. (2006). Structures that contribute to middle-ear admittance in chinchilla, *J. Comp. Physiol. A* 192, 1287-1311.
- [21] Bárány, E. (1938). A contribution to the physiology of bone conduction, *Acta Otolaryngol.*, Suppl. 26, 1-223.
- [22] Békésy, G. von (1960). *Experiments in Hearing*, (McGraw-Hill, New York), Chap 6, 127-203.
- [23] Huizing EH. (1960). Bone conduction- the influence of the middle ear, *Acta Otolaryngol*, Suppl 155.
- [24] Tonndorf, J. (1962). Compressional bone conduction in cochlear models, *J. Acoust. Soc. Am.* 34, 1127-1131.
- [25] Tonndorf, J. (1966). Bone conduction. Studies in experimental animals; A collection of seven papers, *Acta Oto-Laryngol.*, Suppl. 213, 1-132.
- [26] Stenfelt S: Simultaneous cancellation of air and bone conduction tones at two frequencies: Extension of the famous experiment by von Békésy. *Hear Res* 2007;225:105-116.
- [27] Stenfelt S, Puria S, Hato N, Goode RL: Basilar membrane and osseous spiral lamina motion in human cadavers with air and bone conduction stimuli. *Hear Res* 2003;181:131-143.

- [28] Slama MCC. M.S. thesis. Massachusetts Institute of Technology; Cambridge, MA: 2008. Middle ear pressure gain and cochlear input impedance in the chinchilla.
- [29] Wever E.G. and Lawrence M. Physiological acoustics. Princeton, NJ: Princeton University Press, 1954.
- [30] Ravicz, ME, Rosowski, JJ. (2013). Inner-ear sound pressure near the base of the cochlea in chinchilla: Further investigation, *J. Acoust. Soc. Am.* 133 (4), April 2013.
- [31] Décory, L., Franke, R.B., and Daner, A.L. (1990). Measurement of the middle ear transfer function in cat, chinchilla and guinea pig, in *The Mechanics and Biophysics of Hearing*, edited by P. Dallos, C. D. Geisler, J.W. Matthews, M.A. Ruggero, and C.R. Steele (Springer, Berlin), pp. 270-277.
- [32] Nedzelnitsky, V. (1980). Sound pressure in the basal turn of the cat cochlea, *J. Acoust. Soc. Am.* 68, 1676-1689.
- [33] Ravicz, M. E., and Rosowski, J. J. (2012). A New estimate of the middle-ear transmission matrix in chinchilla, in abstracts of the 35th Midwinter Meeting of the Association for Research in Otolaryngology (Association for Research in Otolaryngology, Mt. Royal, NJ), #126 (abstract).